Influence of Pitching Motion on Subsonic Wing Rock of Slender Delta Wings

J. M. Elzebda,* D. T. Mook,† and A. H. Nayfeh‡
Virginia Polytechnic Institute and State University, Blacksburg, Virginia

A numerical simulation of the subsonic wing-rock phenomenon for slender delta wings is described. The present numerical model accounts for a second degree of freedom in pitch. According to the present simulation, there are two onset angles of attack: α_1 and α_2 where $\alpha_1 < \alpha_2$. When $\alpha < \alpha_1$, all initial disturbances decay, and the wing is stable. When $\alpha_1 < \alpha < \alpha_2$, for all initial disturbances, the oscillation in pitch becomes very small, but a large-amplitude limit cycle develops in roll. The rolling motion is virtually identical to the motion for a single degree of freedom in roll. When $\alpha > \alpha_2$, all initial disturbances lead to large-amplitude motions in both roll and pitch. The roll motion in this case differs markedly from the motion for a single degree of freedom. The present results suggest that the motion observed in the wind tunnel for the single-degree-of-freedom case differs significantly from the motion for the two-degree-of-freedom case. The numerical simulation of the wing-rock phenomenon for only one degree of freedom agrees very closely with two sets of experimental observations.

Introduction

MANY modern combat aircraft often operate at subsonic speeds and high angles of attack. At sufficiently high angles of attack, these aircraft become unstable and enter into an oscillatory, mainly rolling motion known as wing rock.[1-5] There have been many efforts to investigate and understand wing rock. Different investigators have given different opinions as to what physical mechanisms cause this phenomenon. Ross[6] proposed that limit cycles occur when either the rolling moment or the yawing moment is cubic with respect to the sideslip angle and that a rolling moment nonlinear in the roll rate may also cause limit cycles.[7] Aerodynamic hysteresis has also been proposed as the cause of limit-cycle motions.[1]

Nguyen et al.[8] tested a flat-plate delta wing with 80 deg leading-edge sweep in a wind tunnel. In the free-to-roll tests, their model exhibited large-amplitude, limit-cycle wing rock at angles of attack greater than 25 deg. From their analysis, they concluded that the dependence of the aerodynamic roll damping on the sideslip causes wing rock. Levin and Katz[9] conducted wind-tunnel experiments similar to those of Nguyen et al., but with different support conditions. Nonlinearities in the rolling moment, vortex asymmetry, and vortex breakdown, as reported by Levin and Katz, caused wing rock. Upon studying the results of Nguyen et al., Ericsson[10] concluded that wing rock is caused by asymmetric leading-edge vortices and never by vortex breakdown. Indeed, vortex breakdown probably has a damping effect on the rolling motion.

Konstadinopoulos[11]; Konstadinopoulos et al.,[12] and Mook and Nayfeh[13] presented a numerical simulation of the experiments described.[8,9] They combined a general method to predict unsteady aerodynamic loads with a numerical integration scheme to predict the motion of the fluid and wing simultaneously and interactively. Their results are in good agreement with the experimental results. The simulation predicted that as the angle of attack increases, the symmetric configuration of the leading-edge vortex system becomes unstable. The loss of symmetry causes a loss of roll damping at small angles of roll. Consequently, any small disturbance introduced into the flowfield grows, and wing rock develops.

Hsu and Lan[4] developed a theory to describe the mechanisms of wing rock. They applied their theory to the experimental data of Nguyen et al.[8] They concluded that wing rock is caused by flow asymmetries, developed by negative or weakly positive roll damping, and sustained by nonlinear aerodynamic roll damping. In 1984, Katz and Levin[14] repeated the experiment they had performed in 1982[9]; however, this time they installed a small canard in front of the delta wing. This experiment emphasized that subsonic wing rock of slender delta wings is caused by dynamic vortex interaction with the lifting surface. They explained how the canard increased the range of angle of attack at which wing rock occurred.

From the above survey it appears that no analytical, experimental, or numerical study has been undertaken to consider the effect of an additional degree of freedom in pitch on the wing rock of slender delta wings.

In the present investigation, a slender delta wing that is free to rotate simultaneously in both roll and pitch is considered. The numerical simulation is based on an extension of the one used by Konstadinopoulos[11] and Konstadinopoulos et al.[12]

For a complete description of the unsteady vortex-lattice method, see Refs. 15 through 18.

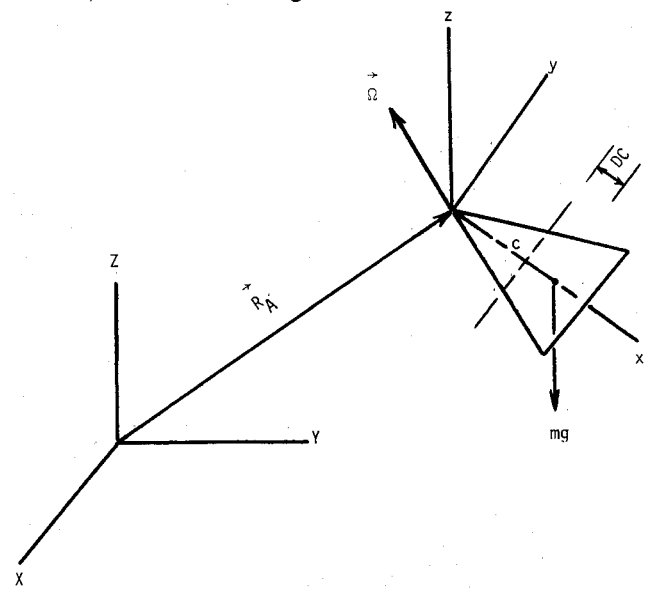

Fig. 1 Schematic of the delta wing used in the numerical simulation (not to scale).

Presented as Paper 87-0496 at the AIAA 25th Aerospace Sciences Meeting, Reno, NV, Jan. 12–15, 1987; received March 31, 1987; revision received Oct. 31, 1987. Copyright © 1988 American Institute of Aeronautics and Astronautics, Inc. All rights reserved.

*Graduate Research Assistant, Department of Engineering Science and Mechanics.

†Professor, Department of Engineering Science and Mechanics. Member AIAA.

‡University Distinguished Professor, Department of Engineering Science and Mechanics. Member AIAA.

Description of the Numerical Procedure

The numerical procedure described here simultaneously predicts the flowfield and the motion of the wing. The aerodynamic loads acting on the wing are obtained by the general unsteady vortex-lattice method (UVLM). The problem is complicated by the fact that to calculate the loads one must know the motion, whereas to calculate the motion one must know the loads. To resolve this dilemma, we use iteration in the present procedure.

Because UVLM is designed to use unit steps in time, the present development is based on a predictor-corrector scheme instead of a Runge-Kutta scheme. The details of the numerical integration are given by Elzebda.[18]

We consider the motion of a uniform, flat, thin wing, supported on a ball-and-socket at point C, as shown in Fig. 1, the same wing used in the experiment.[9] In Fig. 1 there is a reference frame attached to the lifting surface and one attached to the ground. These are called body-fixed (B–F) and ground-fixed (G–F) reference frames, respectively. For any rigid body, the equations of motion have the form

$$M_x = I_{xx}\dot{\Omega}_x + (I_{zz} - I_{yy})\Omega_z\Omega_y \tag{1a}$$

$$M_y = I_{yy}\dot{\Omega}_y + (I_{xx} - I_{zz})\Omega_x\Omega_z \tag{1b}$$

$$M_z = I_{zz}\dot{\Omega}_z + (I_{yy} - I_{xx})\Omega_y\Omega_x \tag{1c}$$

where M_x, M_y, and M_z are the components of the external moment around point C; Ω_x, Ω_y, and Ω_z are the components of the angular velocity of the wing; and I_{xx}, I_{yy}, and I_{zz} are the components of the inertia tensor. With respect to body-fixed axes, all have their origin at point C.

After introducing the Euler angles (ψ,θ,ξ) in the sequence (3,2,1) into Eqs. (1) and noting that

$$I_{zz} \simeq I_{yy} + I_{xx} \tag{2}$$

we can obtain

$$M_x = I_{xx}(\ddot{\xi} - S\theta\ddot{\psi}) + I_{xx}[C\xi S\xi(C^2\theta\dot{\psi}^2 - \dot{\theta}^2) - 2C\theta S^2\xi\dot{\theta}\dot{\psi}] \tag{3}$$

$$M_y = I_{yy}(C\xi\ddot{\theta} + S\xi C\theta\ddot{\psi}) + I_{yy}[S\theta(C\theta C\xi\dot{\psi}^2 - 2S\xi\dot{\theta}\dot{\psi})] \tag{4}$$

$$M_z = I_{zz}(C\xi C\theta\ddot{\psi} - S\xi\ddot{\theta}) + I_{xx}[S\theta C\theta S\xi\dot{\psi}^2 - 2S\xi C\theta\dot{\xi}\dot{\psi} - 2C\xi\dot{\xi}\dot{\theta}] + I_{yy}[-S\theta C\theta S\xi\dot{\psi}^2 - 2C\xi S\theta\dot{\psi}\dot{\theta}] \tag{5}$$

where $C\xi = \cos\xi$, $S\xi = \sin\xi$, etc.

The moments are generated by the aerodynamic forces, whatever small damping there is in the ball and socket, and gravity. The moment due to gravity can be computed as follows:

$$\boldsymbol{M}_G = DC\boldsymbol{i} \times (-mg\boldsymbol{K})$$

where DC is the distance between point C and the center of gravity and $\boldsymbol{K}$ is the unit vector parallel to the vertical direction; $\boldsymbol{K}$ can be written in B–F frame as

$$\boldsymbol{K} = -S\theta\boldsymbol{i} + S\xi C\theta\boldsymbol{j} + C\xi C\theta\boldsymbol{k}$$

Then it follows that

$$\boldsymbol{M}_G = mgDC(C\xi C\theta\boldsymbol{j} - S\xi C\theta\boldsymbol{k}) \tag{6}$$

The damping moment $\boldsymbol{D}$ is written as

$$\boldsymbol{D} = -\mu_x\Omega_x\boldsymbol{i} - \mu_y\Omega_y\boldsymbol{j} - \mu_z\Omega_z\boldsymbol{k}$$

which can be rewritten in terms of the Euler angles as

$$\boldsymbol{D} = -\mu_x(\dot{\xi} - S\theta\dot{\psi})\boldsymbol{i} - \mu_y(C\xi\dot{\theta} + S\xi C\theta\dot{\psi})\boldsymbol{j} - \mu_z(C\xi C\theta\dot{\psi} - S\xi\dot{\theta})\boldsymbol{k} \tag{7}$$

where μ_x, μ_y, and μ_z are the damping coefficients. The aerodynamic moment is

$$\boldsymbol{A} = \frac{1}{2}\rho U_c^2 sc(C_x\boldsymbol{i} + C_y\boldsymbol{j} + C_z\boldsymbol{k}) \tag{8}$$

where ρ is the density of the air; U_c is a characteristic speed; S is the area of the planform; c is the chord; and C_x, C_y, and C_z are the aerodynamic moment coefficients supplied by UVLM.

By substituting Eqs. (6–8) into Eqs. (3–5) and introducing the dimensionless variable $t^* = (U_c/L_c)t$, where L_c is the characteristic length, one can obtain

$$\begin{bmatrix} 1 & 0 & -S\theta \\ 0 & C\xi & S\xi C\theta \\ 0 & -S\xi & C\xi C\theta \end{bmatrix} \begin{Bmatrix} \ddot{\xi} \\ \ddot{\theta} \\ \ddot{\psi} \end{Bmatrix} = \begin{Bmatrix} R_x \\ R_y \\ R_z \end{Bmatrix} \tag{9}$$

where

$$R_x = C_1C_x - C_2(\dot{\xi} - S\theta\dot{\psi}) - C\xi S\xi(C^2\theta\dot{\psi}^2 - \dot{\theta}^2) + 2C\theta S^2\xi\dot{\theta}\dot{\psi} \tag{10}$$

$$R_y = C_3C_y - C_4(\xi\dot{\theta} + S\xi C\theta\dot{\psi}) + C_5C\xi C\theta - S\theta(C\theta C\xi\dot{\psi}^2 - 2S\xi\dot{\theta}\dot{\psi}) \tag{11}$$

$$R_z = C_6C_z - C_7(C\xi C\theta\dot{\psi} - S\xi\dot{\theta}) - C_8S\xi C\theta + 2C_9(S\xi C\theta\dot{\psi} + C\xi\dot{\theta})\dot{\xi} - (C_9 - C_{10})S\theta C\theta S\xi\dot{\psi}^2 + 2C_{10}C\xi S\theta\dot{\psi}\dot{\theta} \tag{12}$$

$$C_1 = \frac{\rho SCL_c^2}{2I_{xx}}, \quad C_2 = \frac{\mu_xL_c}{I_{xx}U_c}, \quad C_3 = \frac{\rho SCL_c^2}{2I_{yy}} \tag{13a,b,c}$$

$$C_4 = \frac{\mu_yL_c}{I_{yy}U_c}, \quad C_5 = \frac{mgDCL_c^2}{I_{yy}U_c^2}, \quad C_6 = \frac{\rho SCL_c^2}{2I_{zz}} \tag{13d,e,f}$$

$$C_7 = \frac{\mu_zL_c}{I_{zz}U_c}, \quad C_8 = \frac{mgDCL_c^2}{I_{zz}U_c^2}, \quad C_9 = \frac{I_{xx}}{I_{zz}}, \quad C_{10} = \frac{I_{yy}}{I_{zz}} \tag{13g,h,i,j}$$

Finally, one can solve Eqs. (9) to obtain expressions for the second derivatives of the Euler angles as

$$\begin{Bmatrix} \ddot{\xi} \\ \ddot{\theta} \\ \ddot{\psi} \end{Bmatrix} = \begin{bmatrix} 1 & S\xi S\theta/C\theta & C\xi S\theta/C\theta \\ 0 & C\xi & -S\xi \\ 0 & S\xi/C\theta & C\xi/C\theta \end{bmatrix} \begin{Bmatrix} R_x \\ R_y \\ R_z \end{Bmatrix} \tag{14}$$

Equations (14) are singular at $\theta = \pm\pi/2$; these values of θ are beyond the range considered here; hence, they do not cause problems.

The numerical procedure described in the previous section is used to predict the response of a slender delta wing to initial disturbances. The properties of the wing are nearly the same as those of the wing used by Levin and Katz[9] in their wind-tunnel experiment. Their experiment considered a wing that was free to roll. Here we consider a wing that is free to roll and pitch. The hinge for rotation in pitch is located so that the wing is in equilibrium at 25 deg angle of pitch (attack) when the air speed is 16.1 m/s. This permits a direct comparison between the numerical results for roll only and the experimental data of Levin and Katz at this angle of attack.

The equations of motion for three degrees of freedom [Eqs. (14)] are reduced as follows: for two degrees of freedom (roll and pitch),

$$\psi \equiv \dot{\psi} \equiv \ddot{\psi} \equiv 0 \tag{15}$$

Then it follows that

$$R_y S\ddot{\xi} + R_z C\ddot{\xi} = 0 \tag{16}$$

Hence,

$$\ddot{\xi} = R_x \tag{17}$$

$$\ddot{\theta} = R_y C\ddot{\xi} - R_z S\ddot{\xi} \tag{18}$$

From Eq. (16) it follows that

$$\ddot{\theta} = R_y / C\ddot{\xi} \tag{19}$$

The quantities R_x, R_y, and R_z are defined in Eqs. (10–12). For this case, R_x reduces to

$$R_x = C_1 C_x - C_2 \dot{\xi} + C\xi S\xi \dot{\theta}^2 \tag{20}$$

and R_y reduces to

$$R_y = C_3 C_y - C_4 C\xi \dot{\theta} + C_5 C\xi C\theta \tag{21}$$

The coefficients are defined in Eqs. (13). We note that C_y is the dimensionless aerodynamic moment about the y axis fixed in the wing. It was predicted by the vortex-lattice method. The boundary conditions for this calculation use the instantaneous position and velocity; thus, when the wing rolls, the actual boundary conditions used correspond to the wing at a reduced angle of attack and in a crossflow (i.e., experiencing sideslip). With the present procedure the reduced angle of attack and the sideslip are already in the C_y; hence, $\cos\xi$ and $\sin\theta$ do not appear explicitly in this term.

For one degree of freedom,

$$\theta \equiv \dot{\theta} \equiv \ddot{\theta} \equiv 0 \tag{22}$$

in addition to Eq. (15) above. Hence, R_x reduces to

$$R_x = C_1 C_x - C_2 \dot{\xi} \tag{23}$$

and ξ is still governed by Eq. (17).

The physical model used in this work has the following properties: Chord = 0.429 m, L_c = chord/4; leading-edge-sweep angle = 80 deg, aspect ratio = 0.705, area = 0.324×10^{-1} m^2, mass = 0.284 kg, $DC = 0.737 \times 10^{-1}$ m, $I_{xx} = 0.27 \times 10^{-3}$ kg-m^2, $I_{yy} = 0.44 \times 10^{-2}$ kg-m^2, $I_{zz} = 0.47 \times 10^{-2}$ kg-m^2, and $\rho_{air} = 0.12 \times 10^{-2}$ kg-m^{-3}.

Levin and Katz[9] gave only the value of I_{xx}. Here we have estimated the corresponding values of mass, I_{yy}, and I_{zz} by assuming the wing to be a thin, flat, uniform plate. (The actual wing had a hump in the center that housed the bearing assembly of the free-to-roll sting.)

Here we consider two angles of attack: $\alpha = 22.5$ deg, an angle for which in essence only roll is excited; and $\alpha = 25$ deg, an angle for which both roll and pitch are strongly excited.

Not presented here are numerical results for $\alpha = 15$ deg and 20 deg. For $\alpha = 15$ deg, the wing is stable, and all initial disturbances decay. For $\alpha = 20$ deg, the wing is borderline unstable. In both cases the additional degree of freedom in pitch has no apparent effect on the motion; the predicted motions are virtually identical to those presented in Ref. 12. The critical angle for the onset of wing rock is not changed by the additional degree of freedom in pitch.

Also not shown here are the results for one degree of freedom in pitch. The numerical simulation shows the wing is stable to all reasonable disturbances.

For $\alpha = 22.5$ deg, we choose the freestream speed to be $U_\infty = 17.2$ m/s and the damping coefficients to be $\mu_x = 0.378 \times 10^{-4}$ and $\mu_y = \mu_z = 0$. For this freestream speed the wing is in equilibrium at 22.5 deg angle of attack. The coefficients in Eqs. (13) become $C_1 = 0.354$, $C_2 = 0.872 \times 10^{-3}$, $C_3 = 0.0215$, $C_4 = 0.0$, and $C_5 = 0.179 \times 10^{-2}$.

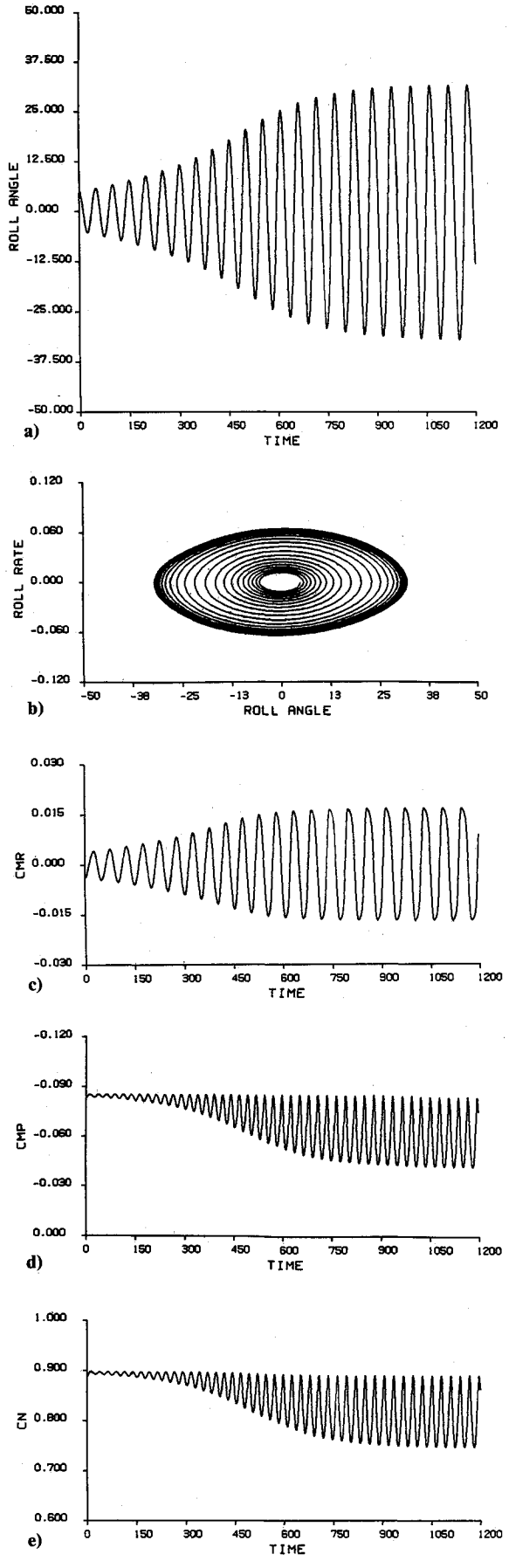

Fig. 2 Numerical results for one degree of freedom in roll, $\alpha = 22.5$ deg; $\xi(0) = 5$ deg; $\dot{\xi}(0) = 0$: a) roll angle as a function of time, b) phase plane, c) roll-moment coefficient, d) pitch-moment coefficient, and e) normal-force coefficient as functions of dimensionless time.

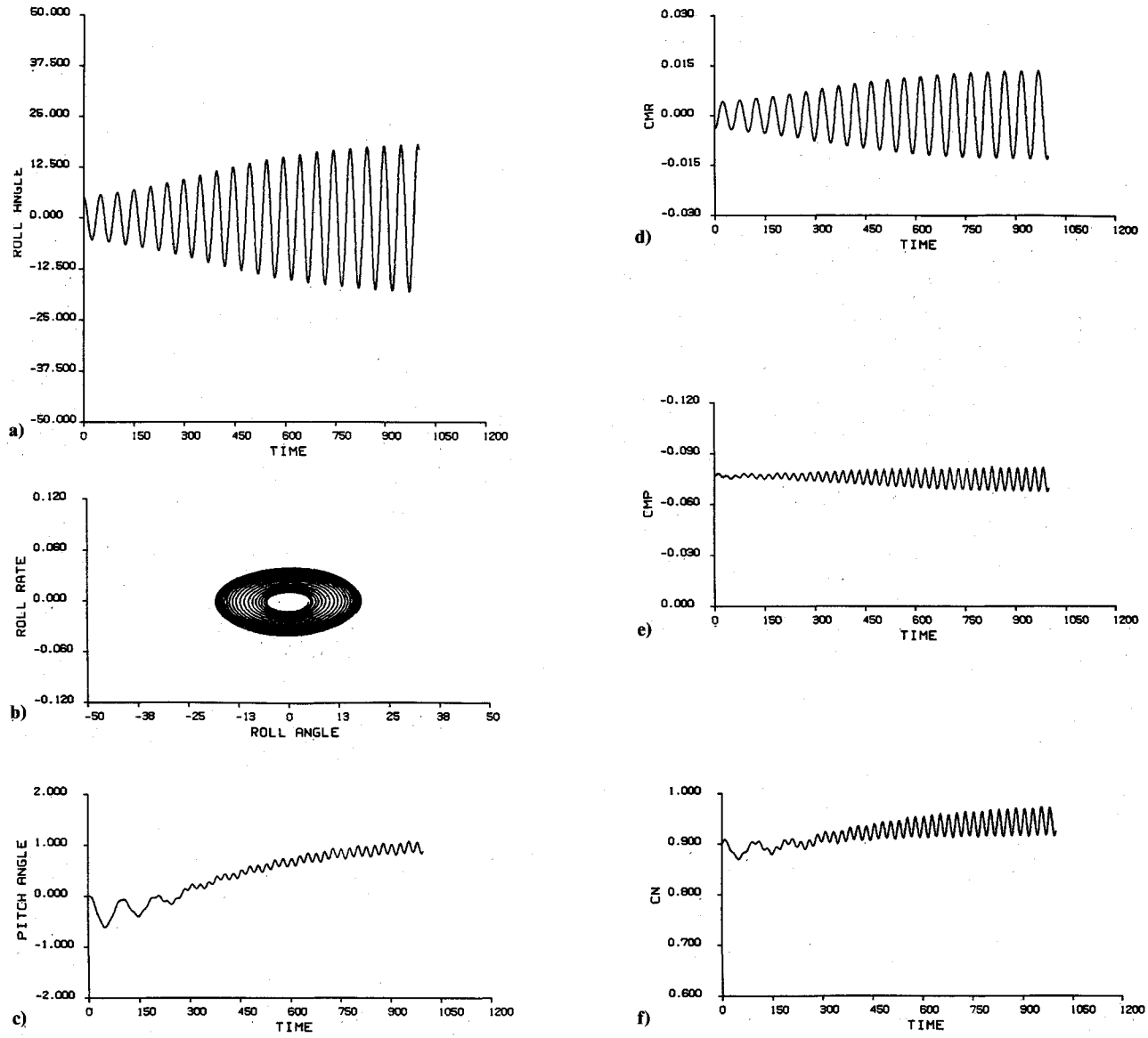

Fig. 3 Numerical results for two degrees of freedom in roll and pitch, $\alpha = 22.5$ deg, $\zeta(0) = 5$ deg, $\dot{\zeta}(0) = 0$: a) roll angle as a function of time, b) phase plane, c) pitch angle, 3) roll-moment coefficient, e) pitch-moment coefficient, and f) normal-force coefficient as functions of dimensionless time.

The results for one degree of freedom in roll are given in Fig. 2. Clearly, the motion rapidly approaches a limit cycle as indicated in part a, where the roll angle is shown as a function of time, and in part b, where the phase plane is shown. The roll moment, pitch moment, and normal force are given as functions of time in parts c, d, and e, respectively. The roll angle and roll moment have the same period but are not in phase. The pitch moment and normal force have one-half the period of the roll angle and roll moment. Moreover, the mean pitch moment significantly increases toward zero, while the mean normal force correspondingly decreases. These results suggest that for two degrees of freedom the wing may pitch up while oscillating in roll.

The results for two degrees of freedom (roll and pitch) are shown in Fig. 3. The motion appears to be approaching a limit cycle, as in the case of one degree of freedom. But here both the amplitude and period are less than those in the case of one degree of freedom. In part c, the deviation in the pitch angle from the equilibrium position is given as a function of time. The mean pitch angle increases by approximately one degree. The roll moment, pitch moment, and normal force are shown in parts d, e, and f, respectively. There appears to be a second onset angle around 22 deg for the onset of pitching motion, because for $\alpha = 20$ deg the motions for one and two degrees of freedom were virtually identical.

Comparing Fig. 2a with Fig. 3a, we find that rather low-amplitude changes in the pitch motions lead to a rather significant reduction in both the growth rate and the amplitude of the roll motion.

For $\alpha = 25$ deg we choose the freestream speed to be $U_\infty = 16.1$ m/s and the damping coefficients to be $\mu_x = 0.378 \times 10^{-3}$, $\mu_y = \mu_z = 0$. The coefficients in Eqs. (13) become $C_1 = 0.354$, $C_2 = 0.933 \times 10^{-3}$, $C_3 = 0.0215$, $C_4 = 0$, and $C_5 = 0.206 \times 10^{-2}$.

The results for one degree of freedom in roll are given in Fig. 4. Clearly, the motion reaches a limit cycle as shown in parts a and b. A comparison of parts a and b of Figs. 2 and 4 shows that the limit cycle is reached more quickly at higher angles of attack. The amplitude of the limit-cycle motion is approximately 33 deg, and the period is approximately 0.4 s. Both agree closely with the observations of Levin and Katz. The roll moment, pitch moment, and normal force are given as functions of time in parts c, d, and e, respectively. The mean values of both the pitch moment and the normal force are less than

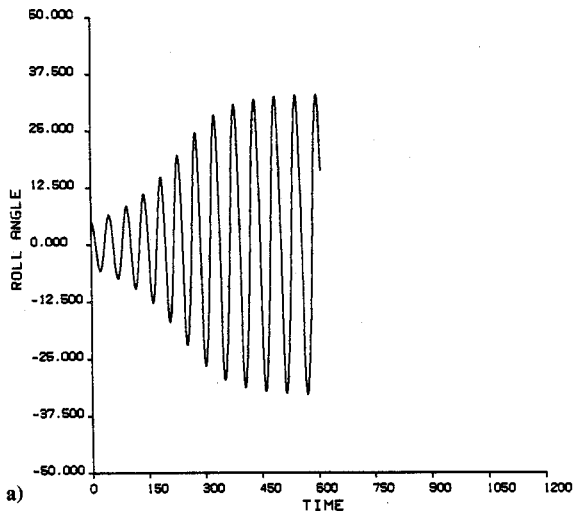

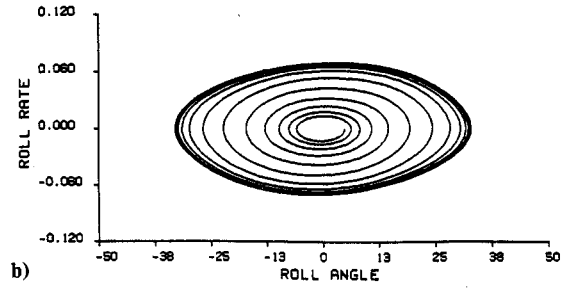

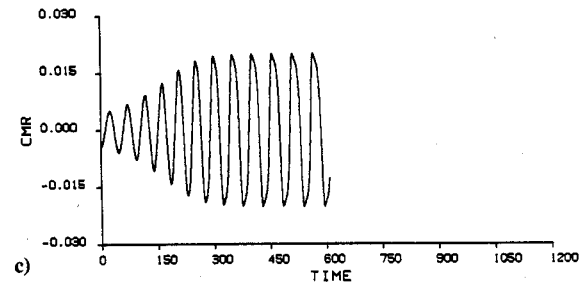

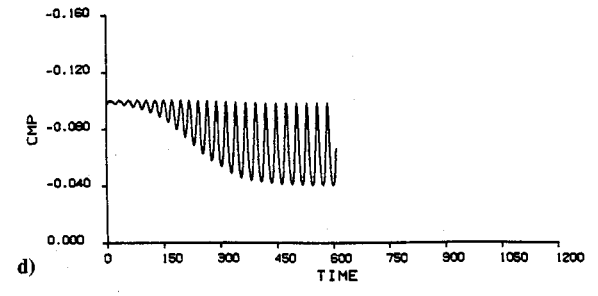

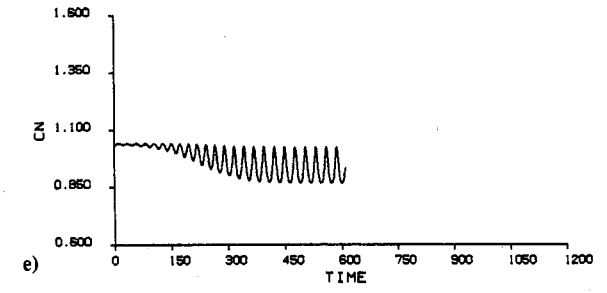

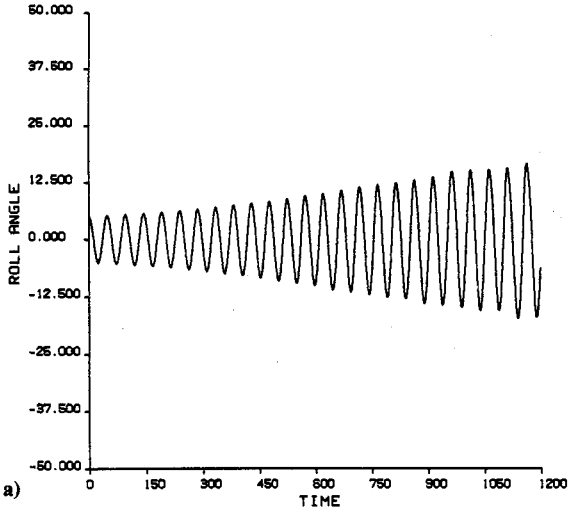

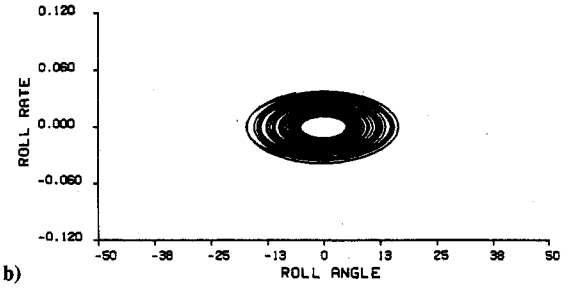

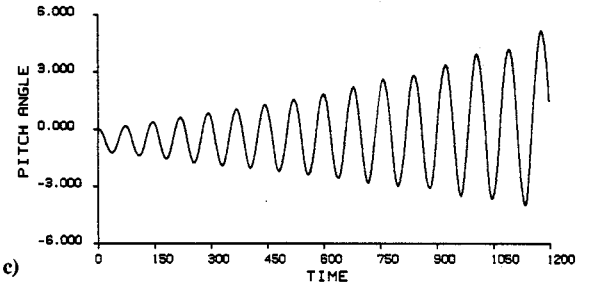

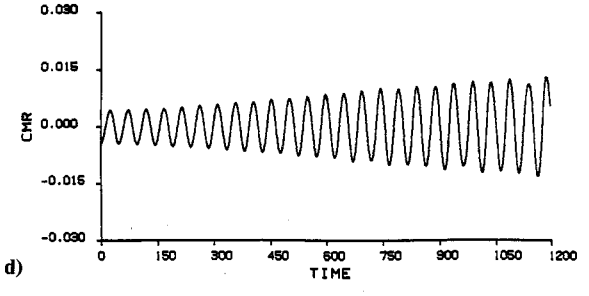

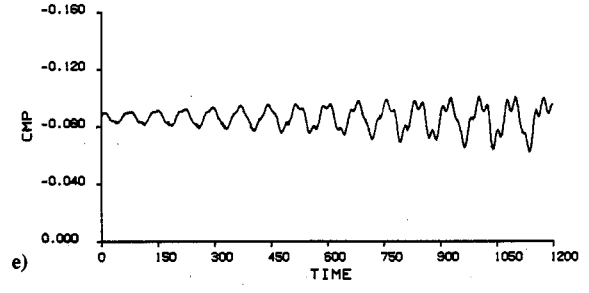

Fig. 4 Numerical results for one degree of freedom in roll, $\alpha = 25$ deg, $\xi(0) = 5$ deg, $\dot{\xi}(0) = 0$: a) roll angle as a function of time, b) phase plane, c) roll-moment coefficient, d) pitch-moment coefficient, and e) normal-force coefficient as functions of dimensionless time.

Fig. 5 Numerical results for two degrees of freedom in roll and pitch, $\alpha = 25$ deg, $\xi(0) = 5$ deg, $\dot{\xi}(0) = 0$: a) roll angle as a function of time, b) phase plane, c) pitch angle, d) roll-moment coefficient, e) pitch-moment coefficient.

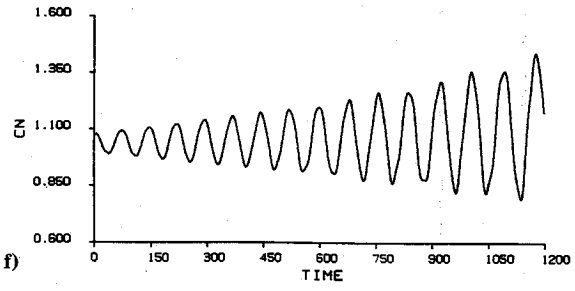

Fig. 5 (con't) Numerical results for two degrees of freedom in roll and pitch, $\alpha = 25$ deg, $\dot{\gamma}(0) = 5$ deg, $\dot{\gamma}(0) = 0$: f) normal-force coefficient as functions of dimensionless time.

those for the static case. This suggests that for two degrees of freedom the wing will pitch up.

The results for two degrees of freedom are given in Fig. 5. In part a, the roll angle is shown as a function of time, and in part b, the corresponding phase plane is shown. Part c gives the pitch angle as a function of time. The roll motion is growing slowly in comparison with the motion in Fig. 4. A limit cycle has not yet developed in Fig. 5, but after 600 time steps the amplitude of the roll motion for two degrees of freedom is only about one third of the amplitude for one degree of freedom. The period in roll is slightly less than that for one degree of freedom. Moreover, the period in pitch is slightly less than twice the period in roll. This suggests, as does the obvious change in amplitude, that transient solutions are still present in the response. The roll motion appears to lose energy to the pitch motion. The roll moment, pitch moment, and normal force are given as functions of time in parts d, e, and f, respectively. The pitch moment clearly appears to have several harmonics; it is not clear yet whether these are numerical aberrations or representative of the actual response.

Conclusions

The present results lead to the following conclusions.

1) Below the first critical angle of attack (approximately 18 or 19 deg), all disturbances decay for both one and two degrees of freedom.

2) The first critical angle appears to be the same for one and two degrees of freedom.

3) For one degree of freedom in roll, when the angle of attack is above the first critical angle, the motion develops a limit cycle. The higher the angle of attack, the faster the limit cycle develops.

4) For two degrees of freedom in roll and pitch, when the angle of attack is above the first critical angle and below the second critical angle (approximately 22 deg), the motion is almost entirely in roll. The deviation in the pitch angle from the static angle of attack is small and has both a steady and an oscillatory component. The mean angle of attack increases slightly. The motions for both one and two degrees of freedom are virtually identical.

5) For two degrees of freedom, when the angle of attack is above the second critical angle, the motion consists of significant roll and pitch components.

6) For two degrees of freedom, the time for a steady state to develop increases rapidly with the amplitude of the static pitch angle. As a result, the amplitude of the roll motion for two degrees of freedom is considerably less than that for one degree of freedom at a given time after the same initial disturbance.

7) For one degree of freedom in pitch, the motion always decays to the static equilibrium position.

8) For two degrees of freedom the predicted motion differs significantly from the observed and predicted motions for one degree of freedom. These results suggest that the roll motion of an actual aircraft could be less severe than the one-degree-of-freedom case indicates; however, so far there has not been an experimental study to confirm this.

Acknowledgement

This work was supported by the Air Force Office of Scientific Research under Grant No. AFOSR–85–0158.

References

[1]Schmidt, L. V., "Wing Rock Due to Aerodynamic Hysteresis," *Journal of Aircraft*, Vol. 16, 1979, pp. 129–133.

[2]Hwang, C. and Pi, W. S., "Some Observations on the Mechanism of Aircraft Wing Rock," AIAA Paper 78–1456, 1978.

[3]Nguyen, L. T., Gilbert, W. P., Gera, J., Iliff, K. W., and Eneroldson, E. K., "Application of High-α Control System Concepts to a Variable Sweep Fighter Airplane," AIAA Paper 80-1582, 1980.

[4]Hsu, C. and Lan, C. E., "Theory of Wing Rock," *Journal of Aircraft*, Vol. 22, Oct. 1985, pp. 920–924.

[5]Maneuver Limitation of Combat Aircraft, AGARD–AR–155A, Aug. 1979.

[6]Ross, A. J., "Investigation of Nonlinear Motion Experienced on a Slender-Wing Research Aircraft," *Journal of Aircraft*, Vol. 9, 1972, pp. 625–631.

[7]Ross, A. J., "Lateral Stability at High Angles of Attack, Particularly Wing Rock," AGARD CP–260, Paper 10, 1979.

[8]Nguyen, L. T., Yip, L., and Chambers, J. R., "Self-Induced Wing Rock of Slender Delta Wing," AIAA Paper 81-1883, 1981.

[9]Levin, D. and Katz, J., "Dynamic Load Measurements with Delta Wings Undergoing Self-Induced Roll-Oscillations," *Journal of Aircraft*, Vol. 21, Jan. 1984, pp. 30–36.

[10]Ericsson, L. E., "The Fluid Mechanics of Slender Wing Rock," *Journal of Aircraft*, Vol. 21, 1984, pp. 322–328.

[11]Konstadinopoulos, P. A., "Numerical Simulation of the Subsonic Wing-Rock Phenomenon," Ph.D. Dissertation, Virginia Polytechnic Institute and State Univ., Blacksburg, VA, 1984.

[12]Konstadinopoulos, P., Mook, D. T., and Nayfeh, A. H., "Subsonic Wing Rock of Slender Delta Wings," *Journal of Aircraft*, Vol. 22, March 1985, pp. 223–228.

[13]Mook, D. T. and Nayfeh, A. H., "Application of the Vortex-Lattice Method to High-Angle-of-Attack Subsonic Aerodynamics," Society of Automotive Engineers TP–851817, 1985.

[14]Katz, J. and Levin, D., "Measurements of Canard-Induced Roll Oscillations," AIAA Paper 1830–CP, 1985.

[15]Nayfeh, A. H., Mook, D. T., and Yen, A., "The Aerodynamics of Small Harmonic Oscillations Around Large Angles of Attack," AIAA Paper 79-1520, 1979.

[16]Konstadinopoulos, P., "A Vortex-Lattice Method for General Unsteady Subsonic Aerodynamics," M.S. Thesis, Virginia Polytechnic Institute and State Univ., Blacksburg, VA, 1981.

[17]Konstadinopoulos, P., Thrasher, D. F., Mook, D. T., Nayfeh, A. H., and Watson, L., "A Vortex-Lattice Method for General, Unsteady Aerodynamics," *Journal of Aircraft*, Vol. 22, Jan. 1985, pp. 43–49.

[18]Elzebda, J. M., "Two-Degree-of-Freedom Wing Rock and Nonlinear Aerodynamic Interference," Ph.D. Dissertation, Virginia Polytechnic Institute and State Univ., Blacksburg, VA, 1986.